IEEE Access
Multidisciplinary | Rapid Review | Open Access Journal

Received November 29, 2019, accepted December 18, 2019, date of publication December 24, 2019,
date of current version January 3, 2020.

Digital Object Identifier 10.1109/ACCESS.2019.2961963

Seismic Observation and Analysis Based on Three-Component Fiber Optic Seismometer

YUE YANG[1], ZHONGMIN WANG[1,2], TIANYING CHANG[1], MIAO YU[2,3], JUNJIE CHEN[4], GUODONG ZHENG[4], AND HONG-LIANG CUI[1,5]

[1]College of Instrumentation and Electrical Engineering, Jilin University, Changchun 130061, China
[2]Zhuhai Renchi Optoelectronics Technology Company, Ltd., Zhuhai 519000, China
[3]Zhongshan Institute, University of Electronic Science and Technology of China, Zhongshan 528402, China
[4]Earthquake Administration Bureau of Jilin Province, Changchun 130117, China
[5]Chongqing Institute of Green and Intelligent Technology, Chinese Academy of Sciences, Chongqing 400714, China

Corresponding authors: Tianying Chang (tchang@jlu.edu.cn) and Junjie Chen (magcn2@sina.com)

This work was supported in part by the Leading Talents of Guangdong Province Program under Grant 00201507, and in part by the State Oceanic Administration of China under Grant 201405026-01.

ABSTRACT We demonstrate a three-component fiber optic seismometer for seismic observation, with no electronics in the sensor probe, but relying exclusively on optical fiber in the form of an unbalanced Michelson interferometer, with state-of-the-art performance characteristics. The fiber optic seismometer system is installed in the seismic observation cave at the Earthquake Administration Bureau of Jilin Province, in Changchun, Jilin, China, and has been operating without interruption for more than a year. Two minor earthquakes of different magnitudes recorded by the three-component fiber optic seismometer are analyzed and discussed in detail from the perspectives of time domain and frequency domain signal quality and fidelity. In addition, the recording results of the fiber optic seismometer are compared with those of the traditional electrical-mechanical seismometer co-located at the observation site. Actual observational results of the seismic events show that the three-component fiber optic seismometer can record the seismic waves clearly, with comparable performance as the conventional seismometer.

INDEX TERMS Optical fiber applications, optical interferometry, seismic measurements, vibration measurement.

I. INTRODUCTION

Traditional seismometers mostly adopt the leaf spring configuration, with a force-balance electro-mechanical feedback, which realize the characteristics of very broadband, high sensitivity, low noise and large dynamic range [1], [2]. Theses conventional seismometers have been successfully used in the worldwide digital seismic networks owing to their unique advantages. For example, the STS-1, STS-2 seismometers produced by Streckeisen and co-workers have been used in GEOSCOPE global seismic observation network in France to observe the earth's self-noise and earthquake events [3], [4]; The flat response to velocity in the frequency range of the very broadband seismometer STS-1 and the broadband seismometer STS-2 are 0.0028 Hz - 10 Hz and 0.01 Hz - 50 Hz, respectively [5]. The STS-2 seismometer has also been used by the Advanced National Seismic System (ANSS) for routine earthquake monitoring in the United States [6]. In addition, the broadband seismometer Guralp CMG-3T and KS-5400 are deployed in the US [7], the STS-1, STS-2 and CMG-1T, CMG-3T series broadband seismometers are also widely used in seismic observation networks in Japan [8]. The Chinese digital seismic network is widely equipped with the very broadband seismometer CTS-1, which has a velocity response range of 0.0083 Hz -50 Hz [9].

Although traditional seismometers all feature high performance after a century's experimental iteration, there are still some undeniable drawbacks, such as their stringent requirement on the operating environment, their vulnerability to electromagnetic interference, and their need for long-term continuous power supply [10]. Because of such limitations, they have been known to suffer lightning damages in the field, and they cannot be readily deployed in deep boreholes. As a new generation seismometers, optical fiber geophones, combining the advantages of immunity to electromagnetic interference, small footprint, easy multiplexing [11], [12],

The associate editor coordinating the review of this manuscript and approving it for publication was Sukhdev Roy.

and with the sensor probe completely electricity-free, circumvent the problems faced by traditional seismometers elegantly, and as such, has received increasing attention in recent years. The fiber optic seismometer uses no electronics in the sensor probe, rather it relies on fiber optics. It transduces the position of mass by laser interference and reflects the ground vibration information, instead of measuring electromagnetic force required to maintain the inertia mass in place, as is done in almost all broadband seismometers. Additionally, the advantages of high sensitivity, wide dynamic range and mechanical simplicity of optical fiber sensors can outweigh the disadvantages of the open-loop design of most fiber optic seismometers.

The fiber optic seismometer has attracted the attention of many researchers since it was first proposed in the 1990s [13], and has rapidly expanded its designs and applicability in the past decades. Kamenev *et al*. reported a fiber-optic seismometer on the basis of Mach-Zehnder interferometer, where the sensing element of the seismometer was implemented as a multiturn optical coil [14]. Zeng *et al*. reported a mass-loaded mandrel fiber optic accelerometer designed for well-logging seismic observation, and the accelerometer can accomplish the 3-component measurement by multiplexing the three unidirectional sensing elements [15]. Zumberge *et al*. reported a modified STS1 vertical seismometer, whose electronics was replaced with an bulk optical interferometer, and recorded the 2008 Sichuan earthquake [16]; recently, they also reported a completely new three-component borehole optical seismic and geodetic sensor, which was installed at the Albuquerque Seismological Laboratory (ASL) for one year, and had provided geodetic records [17]. Zhang *et al*. reported a fiber optic seismometer based on phase-shifted fiber Bragg grating (FBG), and had recorded short-range small earthquake [18].

Although several previous studies have successfully developed optical fiber seismometers based on various structures, most of them only stay in the laboratory, without actual long-term seismic observation and recording earthquake events. In the work reported here, we developed and deployed a three-component all-optical seismometer based on Michelson interferometer. The seismometer has been installed in a cave in Changchun Jingyue Earthquake Station in Jilin Province, China, since May 2017. The early part of deployment was for the preliminary tests, and the continuous data recording period presented here has been more than one-year long. During this period, the fiber optic seismometer has successfully recorded two earthquake events which are in good agreement with the traditional seismometer co-located in the same observation cave.

The remainder of this report is organized as follows. In Section II, we briefly introduce the working principle of the three-component optical fiber seismometer and the technical performance parameters of the seismometer system. Section III presents the installation and deployment environment of the field seismic observation of the seismometer. In Section IV, the observation results of two earthquakes with different magnitudes are discussed in detail. In Section V, we compare and analyze the results of seismic events recorded by the optical fiber seismometer and the traditional seismometer. Finally, Section VI contains a few concluding remarks.

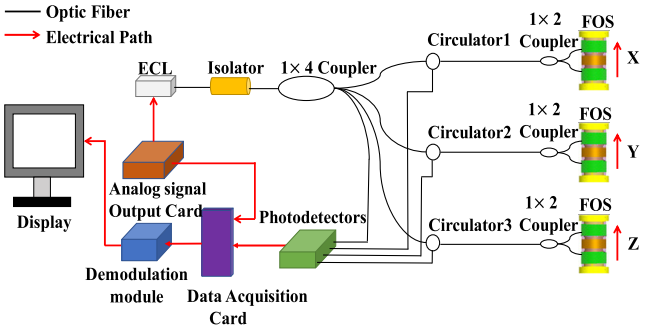

FIGURE 1. Schematic diagram of the three-component fiber optic seismometer. ECL: External cavity laser.

II. THREE-COMPONENT FIBER OPTIC SEISMOMETER

The three-component fiber optic seismometer we developed is based on an unbalanced Michelson interferometer, and the schematic diagram is shown in Fig. 1. The external-cavity laser (ECL) as the light source is modulated by a sinusoidal signal with the frequency of $f_c = 16$ kHz by changing the driving current of the laser. The center wavelength of the ECL is 1550 nm, and the modulated signal is from the analog signal output card, which also outputs octave signals of the fundamental and second harmonic of the modulation frequency. The output of the laser is equally divided into four channels by a 1 x 4 coupler after passing through the isolator used to block the interference signal formed by the reflected light from the Faraday mirrors so as not to affect the laser. The first three light paths pass through the same optical path to ensure the consistency of the three components of the seismometer, which are the circulator and the 1 x 2 coupler for dividing the optical path into two paths again, and enter the corresponding three-component sensing probes, respectively. The light reflected from the Faraday mirror in the transduction probe interferes at the 1 x 2 coupler and outputs at the c end of the circulator. Another function of the Faraday mirror here is that it can eliminate the polarization fading at the end of the interferometer [19]. The four paths are detected by the photodetector and sent to the demodulation module through the data acquisition card. Finally, the display shows the demodulated vibration information.

The sensor probes, adopting the general compliant cylinder structure [20], [21], consist of two fiber-wrapped silicone rubber cylinders, which support a single seismic mass, each wrapped with the optical fiber which acts as one arm of the fiber optic interferometer. The optical fiber acts as both a transmission element and a sensing part in this seismometer. When the external vibration causes a relative displacement of the mass, the motion will cause tension strain to lengthen one of the rubber cylinders and compression strain to shorten

the other, form a push-pull mass-spring system. The optical fiber wrapped around the mandrel will also become longer and shorter together, so the light transmission path between the two interference arms changes, forming the interference. By demodulating this interference signal, one can obtain the vibration information. The symmetrical push-pull structure can not only improve the sensitivity by using the Michelson interferometer, as the light passes through each sensor coil twice, but also reduce the influence of temperature fluctuation and other noises of the system. The height of the sensing probe of the optical fiber seismometer designed by us with the cylindrical shape is 90 mm, and the diameter of the cylinder is 75 mm, it has the advantages of small size and light weight.

The performance parameters of the system are as follows: the average sensitivity of the geophone is 57 dB re rad/g within the operation frequency range 0.005 Hz – 50 Hz; the axial sensitivity is 30 dB higher than the transverse sensitivity; the minimum detectable acceleration level is 50.56 ng/$\sqrt{\text{Hz}}$; the dynamic range of the seismometer is 117.03 dB. Other detailed information on the system design and the performance parameters of the three-component fiber optic seismometer can be obtained from our earlier reports [22]–[25]. Due to the excellent performance of the three-component optical fiber seismometer, it is deemed suitable for practical seismic observation.

III. FIELD DEPLOYMENT

The three-component optical fiber seismometer system was installed in the Changchun Jingyue Seismic Station, Jilin Province, China, where the seismic observatory is equipped with the very broadband seismometer CTS-1. The force balance electronic mechanical feedback system is adopted in this traditional seismometer, which produces the force to keep the mass relatively static through the current feedback coil magnet structure. The seismometer CTS-1's main technical performances can be summarized with the following specifications: the flat to velocity range is 0.0083 Hz - 50 Hz; the sensitivity is 2 × 1000 V/m/s; the maximum ground motion input amplitude is 1.0×10^{-2} m/s; the dynamic range is more than 140 dB [9]. The seismometer CTS-1 is placed on the bedrock inside the cave to observe seismic activities, as shown in Fig. 2 (a).

The optical fiber seismometer system is placed in the seismic observation cave for observing seismic waves in the neighboring chamber, which is isolated from the external environment by 4 levels of waterproof and sound-proof doors. A photograph of the setup for the fiber optic seismometer in the observation cave is shown in Fig. 2 (b). The temperature and humidity of the cave are maintained at approximately 12 °C and 60% throughout the year. The three components of the optical fiber seismometer are fixed in three orthogonal directions (X-North, Y-East, and Z-Vertical) on the bedrock with clay according to the direction indicated on the bedrock.

Specially, the clay can indurate below 20 °C. The host computer contains the electronic-control parts and the optical parts of the system. The display is to show the acceleration

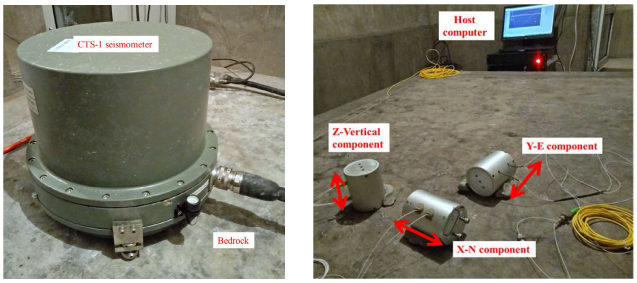

(a) (b)

FIGURE 2. (a) Conventional seismometer CTS-1 installed in the seismic observation station. (b) Setup for optical fiber seismometer in the observation cave.

of the seismic wave in real time, and replay the past test data which is saved on the local disk mounted on the host computer. After installation and an initial testing, the fiber optic seismometer system has been operating continuously with no interruption for more than one year.

IV. SEISMIC OBSERVATION RESULTS

A. OBSERVATION OF THE FIRST SEISMIC EVENT

During the optical fiber seismometer observation period, we first recorded an earthquake event, which occurred on May 18, 2019, in Songyuan, Jilin Province, China. According to the China Seismological Network, the magnitude of the earthquake was 5.1 and the focal depth is 10 km. The time domain information of seismic recording results by the fiber optic seismometer are shown in Fig. 3.

Fig. 3 (a), (b), and (c) are the three orthogonal components (X-North, Y-East, and Z-Vertical) observation results in terms of acceleration versus time, respectively. From Fig. 3, we can see that the P-wave and S-wave of the earthquake can be clearly distinguished from the seismogram for determining the distance of the earthquake, and the arrival time interval between the P-wave and S-wave of the seismic wave is 22.0 s for the north-south direction (Fig. 3 (a)), 22.0 s for the east-west direction (Fig. 3 (b)), and 21.8 s for the vertical direction (Fig. 3 (c)). Moreover, the arrival time of the P-wave measured by the three probe sensors is consistent; the same is true with the S-wave. We can conclude that the consistency of the three-component sensor probes of the fiber optic seismometer is working as designed. The maximum acceleration amplitudes of the S-wave in the three components are 210 μg, 165 μg, 62 μg respectively. Therefore, we can also conclude that the vibration amplitude felt in the vertical direction of an earthquake is the smallest.

In addition, we analyze the frequency domain information of this seismic record of the three components as shown in Fig. 4, which is the amplitude of different frequency components' changes with time. The values corresponding to different colors in Fig. 4 represent the magnitude of acceleration values expressed in dB after normalization. By observing the time-frequency diagram, we can see more intuitively the arrival time and frequency components of the seismic wave.

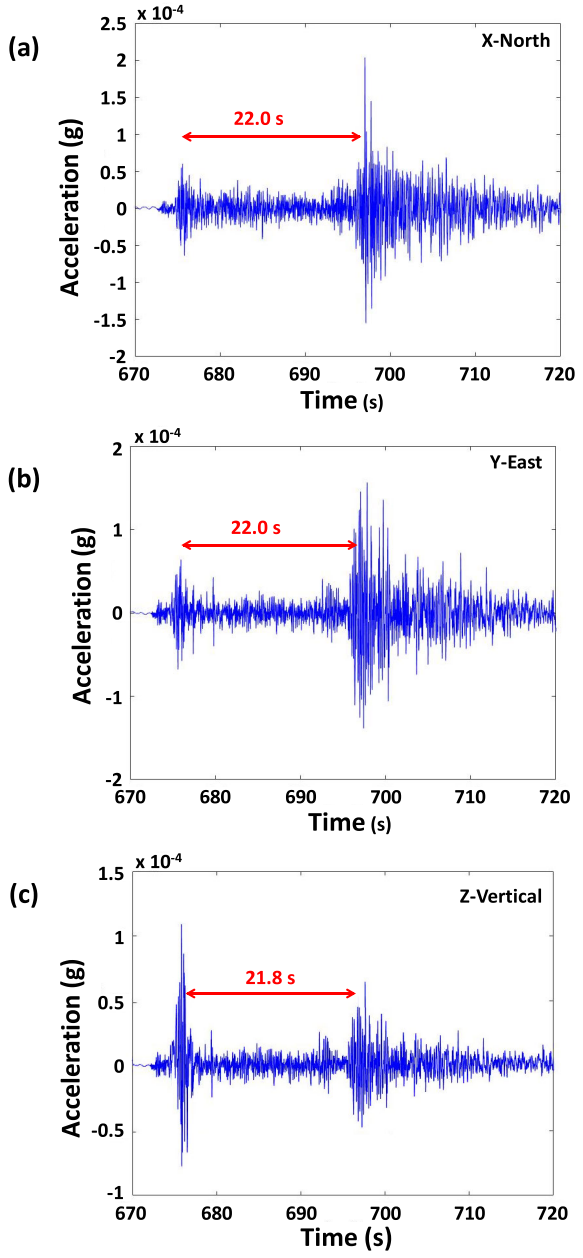

FIGURE 3. An M 5.1 seismic observation in time domain with the fiber optic seismometer: (a) observation result in X-North component, (b) observation result in Y-E component, (c) observation result in Z-Vertical component.

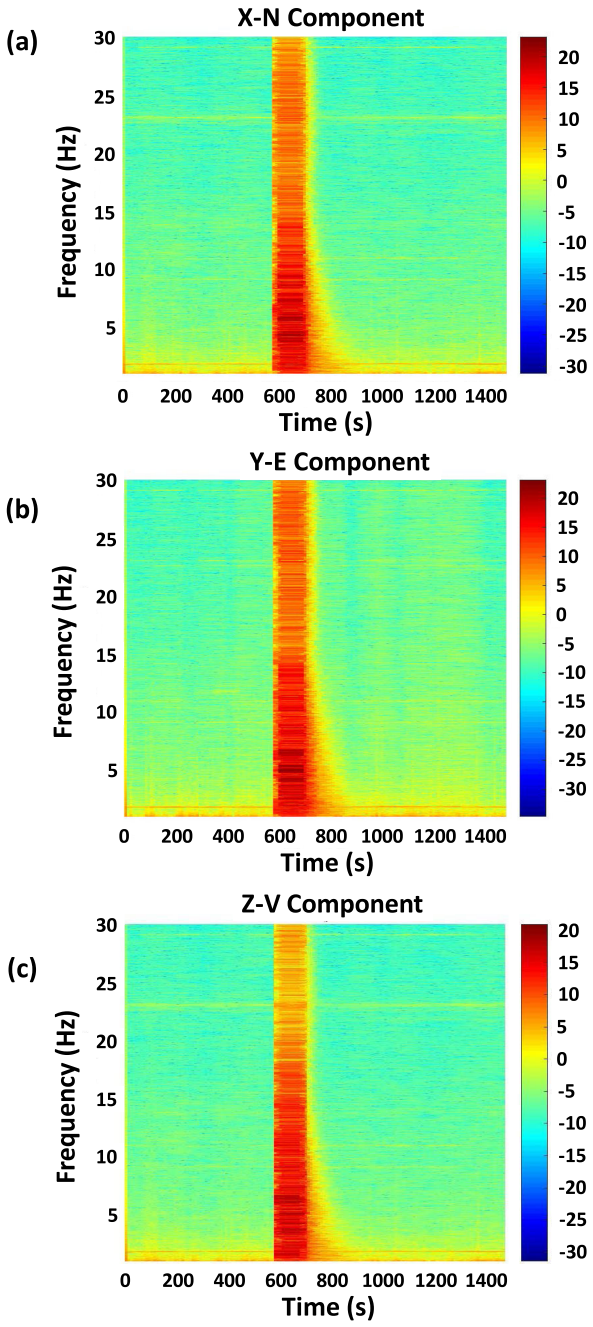

FIGURE 4. An M 5.1 seismic observation in frequency domain with the fiber optic seismometer: (a) observation result in X-North component, (b) observation result in Y-E component, (c) observation result in Z-Vertical component.

From Fig. 4 (a)-(c), we see that the seismic wave recorded by the three components of the fiber optic seismometer contains the same frequency component, and the duration of the seismic wave is all about 120 s above 15 Hz; and with the decrease of frequency, the duration of seismic wave is longer below 15 Hz, the longest time is about 300 s at 0.01 Hz. In particular, the energy is mainly concentrated in the low-frequency band below 15 Hz: as the frequency decreases, the amplitude of the acceleration caused by the seismic wave increases. By comparison between Fig. 4 (a), (b), and (c), it is seen that the acceleration amplitude of the vertical component (Z-Vertical) in the frequency band above 17 Hz is smaller than those of the other two components (X-North, Y- East), while the acceleration amplitudes of the frequency components of the north-south component (X-North) and the east-west component (Y-East) are basically the same.

B. OBSERVATION OF THE SECOND SEISMIC EVENT

Songyuan is an earthquake-prone area due to both anthropogenic and natural causes (a large-scale oil field and active

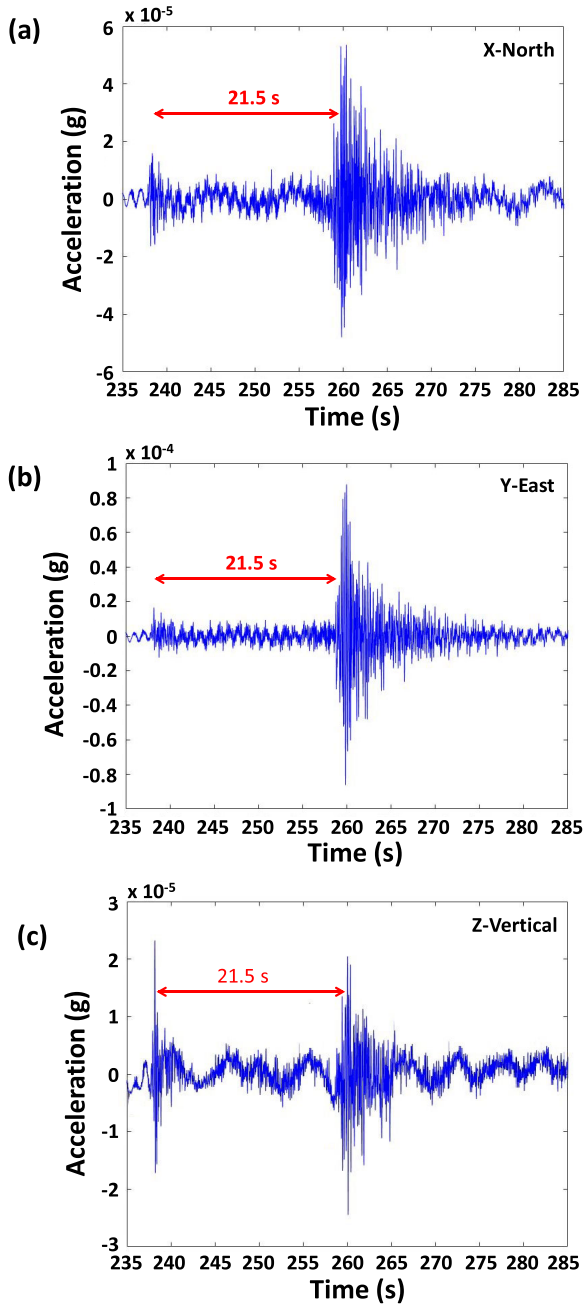

FIGURE 5. An M 4.0 seismic observation in time domain with the fiber optic seismometer: (a) observation result in X-North component, (b) observation result in Y-E component, (c) observation result in Z-Vertical component.

shale gas extraction by hydro-fracking in the environs), thence, we soon recorded another earthquake in Songyuan, Jilin Province, China. It occurred on Jun 03, 2019, the magnitude of the earthquake was smaller than that of the first one, at 4.0, with the focal depth of 12 km. The time-domain information of the seismic observation results are shown in Fig. 5. As can be seen from Fig. 5, the three sensing probes of the optical fiber seismometer still show good consistency in this smaller magnitude earthquake (note that earthquakes are graded on a logarithmic scale), and the time intervals of the P-wave and S-wave of the seismic wave measured by the three orthogonal components are all 21.5 s. By comparing Fig. 5 (a)-(c) showing the three components (X-North, Y-East, and Z-Vertical), we can see that the arrival time of the P-wave measured by the three components is consistent, and the same can be said about the S-wave also. Furthermore, the maximum acceleration amplitudes of the S-wave for the three components are 58 μg, 90 μg, 20 μg, respectively. Similarly, it turns out that the amplitude of the shock felt in the vertical direction is the smallest in an earthquake.

We also analyze this earthquake from the perspective of frequency domain as shown in Fig. 6, which is the change of amplitude of different frequency components of the seismic observation results with time. The values corresponding to different colors in Fig. 6 represent the magnitude of acceleration values expressed in dB after normalization. By comparison between Fig. 6 (a), (b), and (c), we can see that the frequency components of the seismic waves observed by the three orthogonal components are still the same in this small magnitude earthquake, and the change time of the acceleration amplitude caused by the seismic waves is the same. However, it should be noted that this seismic wave lasted for the same time in the full frequency band, about 120 s, which is different from the first earthquake. Similarly, the energy of the seismic wave is mainly concentrated in the low frequency band below 15 Hz. The lower the frequency, the larger the acceleration amplitude. Comparing (a) and (b) in Fig. 6, we can see that the change of acceleration amplitude caused by the seismic wave in the X-North component and the Y-East component are basically the same in the whole frequency band. However, comparing (a) and (c) in Fig. 6, we find that the seismic wave is relatively weak in the Z-Vertical direction, and the change of acceleration amplitude caused is relatively small.

Through the comparative analysis of these two earthquakes with different magnitudes, we can draw a conclusion that the vibration frequency and amplitude of the East-West and North-South orthogonal directions are basically consistent in one earthquake. However, the same frequency component is felt in the vertical direction, but the vibration amplitude caused by the seismic wave is relatively small, which can be clearly seen from the frequency domain that the high frequency band above 15 Hz, where this is particularly obvious. Moreover, as the magnitude decreases, the vibration amplitude decreases not only in the high frequency band but also in the low frequency band. In addition, the duration of the low-frequency component below 15 Hz in the seismic wave increases with the increase of the magnitude, while the duration of the high-frequency component above 15 Hz does not change with the magnitude. It should be specially stated that the above conclusions are only obtained for the two earthquakes discussed in this paper, which have different magnitudes but occurred at the same location. Additionally, in the frequency domain analysis of the second earthquake, by observing the noise background color value in Fig. 6,

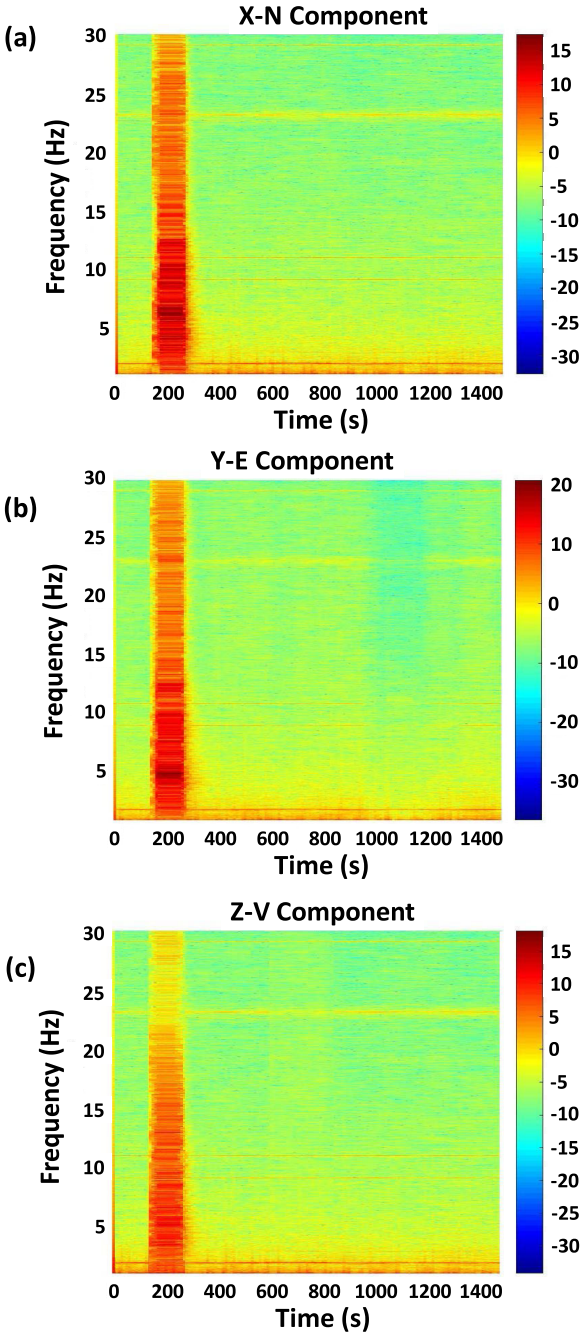

FIGURE 6. An M 4.0 seismic observation in frequency domain with the fiber optic seismometer: (a) observation result in X-North component, (b) observation result in Y-E component, (c) observation result in Z-Vertical component.

we seem to feel that the noise background of the system has become larger, but the noise background of the actual system has not changed. This is because the color display is shown according to the value of the normalized acceleration. In the second earthquake, the amplitude of acceleration became smaller, while the constant noise made the signal-to-noise ratio of the system decrease, so the relative value of the normalized noise increases.

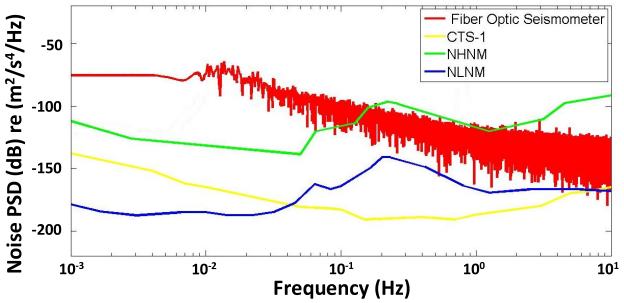

FIGURE 7. Acceleration noise PSD of fiber optic seismometer, CTS-1, NLNM, NHNM.

V. COMPARISON WITH TRADITIONAL SEISMOMETER OBSERVATION RESULTS

We are fortunate to have access to the seismic observation results of the traditional very broadband seismometer CTS-1 about the above two earthquakes with the support of the Changchun Jingyue Seismic Station. Before comparing with traditional seismometer observation results, we compare the acceleration noise of optical fiber seismometer to the seismometer CTS-1, the U.S. Geological Survey's New Low Noise Model (NLNM) and New High Noise Model (NHNM), four acceleration noise power spectral density (PSD) curves with different colors are shown in Fig. 7. NLNM and NHNM are the standard global noise models established by the U.S. Geological Survey, which are commonly accepted as global references. They are the average low and high seismic background noise power spectra obtained from a worldwide network of seismograph stations, and have been taken as baselines for evaluating and comparing station site characteristics, for defining instrument specifications, and for predicting the response of sensor systems under quiet and noisy background conditions. We can see from Fig. 7 that although the acceleration noise of the fiber optic seismometer is somewhat higher than that of the seismometer CTS-1, it is lower than NHNM in the frequency band above 0.1 Hz.

Because the standard seismic data of the Seismological Bureau shows velocity information, hence we converted the raw acceleration signals recorded by the three components optical fiber seismometer into the ground velocity by an integral operation for comparison with the standard CTS-1 seismometer. Fig. 8 is the seismic recordings of the two earthquakes in Songyuan, Jilin Province, China: (a) the magnitude 5.1 earthquake and (b) the magnitude 4.0 event. The plot shows comparisons of the time series from the optical fiber seismometer three components (X-North, Y-East, and Z-vertical) and the conventional CTS-1 seismometer three components sited in the neighboring chamber. In each panel as shown in Fig. 8, the upper seismogram (the blue trace) is the record of the fiber optic seismometer and the lower trace (the red trace) is the record of the conventional CTS-1. Each trace is offset vertically for clarity and the differences of velocity amplitude between the two seismometers is plotted as the center traces (the green trace).

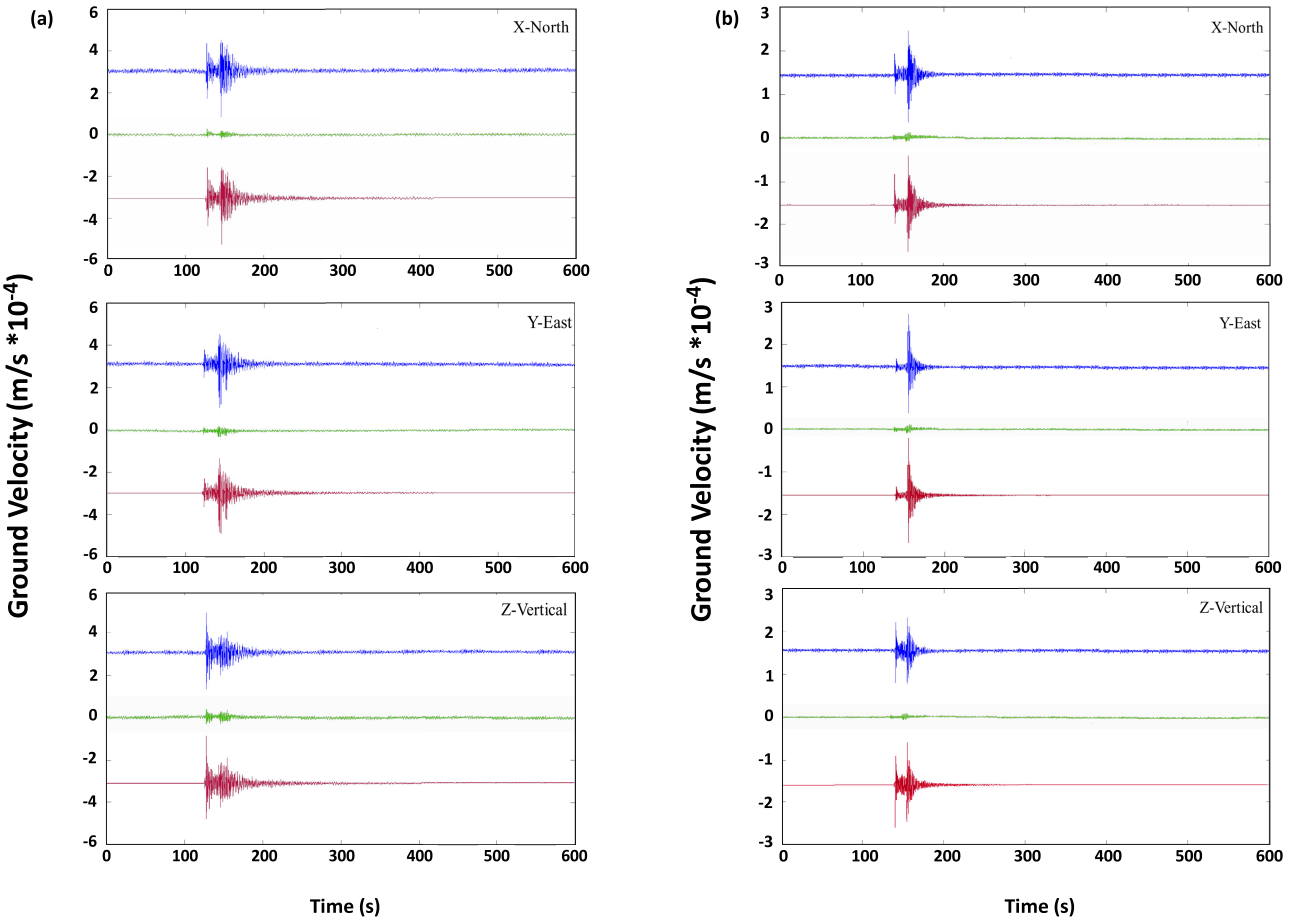

FIGURE 8. Seismograms of the two seismic events in Songyuan: (a) an M 5.1 earthquake, and (b) an M 4.0 earthquake, plotted versus time. The time axis begins at 06: 23 for (a) and 01: 45 for (b). Blue traces: fiber optic sensor output; Red traces: conventional seismometer output; Green traces: the difference between the two.

We can see from the comparison results in Fig. 8 that the waveforms measured with the conventional seismometer and the optical seismometer agree very well and the waveform shapes are nearly identical for the two seismic events. In the two earthquakes, the arrival times of the P-waves detected by the three components of the fiber optic seismometer and the traditional seismometer CTS-1 are the same, and the time intervals of the P-wave and the S-wave recorded are also consistent. In the first seismic event, comparing the optical fiber seismometer and the traditional seismometer, the differences of the maximum velocity amplitude caused by the S-wave in the three components (X-North, Y-East, and Z-vertical) are 0.81%, 1.12%, and 1.34%, respectively. In the second seismic event, the differences are 0.87%, 1.09%, and 0.75%, respectively. We can see from the trace of difference in Fig. 8 that the velocity amplitude obtained by the fiber optic seismometer has a small difference from the velocity amplitude measured by the traditional seismometer, and the largest difference occurs in the vertical component of the first earthquake, but the difference is only 1.34%. Moreover, the error mainly comes from the calculation error introduced in the process of converting the acceleration measured by the fiber optic seismometer into velocity. The only downside is that the noise level of the three-component optical fiber seismometer is higher than that of the traditional standard seismometer CTS-1 as can be seen from Fig. 8. The main reason is that the seismometer sensor probes and the instrumentation box which is connected to the sensor probes by single mode fiber and contains all the electronic parts of the system, including the laser and the photodetectors, are placed in the same room due to resource constraints. The difference in noise performance can be greatly reduced if the optical fiber sensing probes are placed separately from the instrumentation box of the seismometer. Fortunately, we have been able to do just that recently, and have observed a more than 10 dB reduction in noise as a result. We are optimistic that this should bode well for future seismic observation data from our system. Looking at the comparison of seismic event records, this implies that the proposed three-component optical fiber seismometer may have a promising application prospect in the field of earthquake monitoring.

VI. CONCLUSION

We have developed a three-component fiber optic seismometer that relies on optics inside the sensor probe rather than electronics and field-tested it for more than one year in a

seismic observation station. It performed as well as a conventional seismometer, and showed good consistency compared to the traditional high-performance seismometer CTS-1. The operation principle of the fiber optic seismometer system and the sensing mechanism of the sensing probe are briefly discussed. We mainly focus on the detailed analysis of the field seismic observation of the seismometer. Two earthquakes with different magnitudes are analyzed and discussed in detail from two different perspectives of time domain and frequency domain. In addition, we also compare the seismic observation results with those of the traditional seismometer, which shows good consistency.

Through the above demonstration and elaboration, it is hoped to make the case that the optical fiber seismometer can be used for seismic observation. In the future, the three-component fiber optic seismometer will continue to be installed in the seismic observation caves to observe earthquakes in real time, and continuously provide data for analysis and comparison at any time. A more tantalizing prospect is that the sensor can be deployed in deep boreholes and in other harsh environment, where traditional seismometers have encountered debilitating problems.

ACKNOWLEDGMENT

The authors are grateful to the staffs at the Earthquake Administration Bureau of Jilin Province, for allowing the use of their facility and providing data support.

REFERENCES

[1] E. Wielandt and G. Streckeisen, "The leaf-spring seismometer: Design and performance," *Bull. Seismological Soc. Amer.*, vol. 72, no. 6A, pp. 2349–2367, 1982.
[2] M. J. Usher, R. F. Burch, and C. Guralp, "Wide-band feedback seismometers," *Phys. Earth Planet. Interiors*, vol. 18, no. 2, pp. 38–50, Feb. 1979.
[3] M. Vallée, D. Zigone, S. Bonaimé, J.-Y. Thoré, F. Pesqueira, C. Pardo, A. Bernard, E. Stutzmann, A. Maggi, V. Douet, J. Sayadi, and J.-J. Lévêque, "Recent evolutions of the GEOSCOPE broadband seismic observatory," in *Proc. 19th EGU Gen. Assembly Conf. Abstr.*, Apr. 2017, p. 15087.
[4] G. V. Roult, J.-P. Montagner, B. Romanowicz, M. Cara, D. Rouland, R. Pillet, J.-F. Karczewski, L. Rivera, E. Stutzmann, and A. Maggi, "The GEOSCOPE program: Progress and challenges during the past 30 years," *Recent Develop. World Seismol.*, vol. 81, no. 3, pp. 427–452, Jun. 2010.
[5] *USArray A Continental-Scale Seismic Observatory*. [Online]. Available: http://www.usarray.org/researchers/instrumentation/sensors
[6] D. E. Mcnamara, R. P. Buland, and H. M. Benz, "An assessment of the high-gain streckeisen STS2 seismometer for routine earthquake monitoring in the United States," U.S. Geological Survey, Reston, VA, USA, Open-File Rep. 20051437, 2005.
[7] L. C. Holcomb and C. R. Hutt, "Test and evaluation of the Guralp systems CMG-3S broadband borehole deployable seismometer system," U.S. Geological Survey, Reston, VA, USA, Open-File Rep. 91282, 1991.
[8] Y. Okada, K. Kasahara, S. Hori, K. Obara, S. Sekiguchi, H. Fujiwara, and A. Yamamoto, "Recent progress of seismic observation networks in Japan —Hi-net, F-net, K-NET and KiK-net—," *Earth Planets Space*, vol. 56, no. 8, pp. 15–28, Aug. 2004.
[9] C. Yaxian, L. Yongqing, Z. Yunyao, and C. Junling, "CTS-1 very broadband seismometer," *J. Geodesy Geodyn.*, vol. 24, no. 3, pp. 109–114, Aug. 2004.
[10] J. Chen, Y. Yang, W. Gao, T. Chang, and H.-L. Cui, "High sensitivity optical fiber interferometric accelerometer for seismic observation," in *Proc. 26th Int. Conf. Opt. Fibre Sensors*, Lausanne, Switzerland, 2018.
[11] B. Lee, "Review of the present status of optical fiber sensor," *Opt. Fiber Technol*, vol. 9, no. 2, pp. 57–79, Apr. 2003.
[12] F. Peng, Y. Lv, H. Li, S. Tian, W. Chen, and J. Yang, "Sensitivity prediction of multiturn fiber coil-based fiber-optic flexural disk seismometer via finite element method analysis," *J. Lightw. Technol.*, vol. 35, no. 18, pp. 3870–3876, Sep. 15, 2017.
[13] D. L. Gardner, T. Hofler, S. Baker, R. Yarber, and S. Garrett, "A fiber-optic interferometric seismometer," *J. Lightw. Technol.*, vol. 5, no. 7, pp. 953–960, Jul. 1987.
[14] O. T. Kamenev, Y. N. Kulchin, Y. S. Petrov, R. V. Khiznyak, and R. V. Romashko, "Fiber-optic seismometer on the basis of Mach-Zehnder interferometer," *Sens. Actuators A, Phys.*, vol. 244, pp. 133–137, Jun. 2016.
[15] N. Zeng, C. Z. Shi, M. Zhang, L. W. Wang, Y. B. Liao, and S. R. Lai, "A 3-component fiber-optic accelerometer for well logging," *Opt. Commun.*, vol. 234, nos. 1–6, pp. 153–162, 2004.
[16] M. Zumberge, J. Berger, J. Otero, and E. Wielandt, "An optical seismometer without force feedback," *Bull. Seismol. Soc. Amer.*, vol. 100, pp. 598–605, Apr. 2010.
[17] M. Zumberge, J. Berger, W. Hatfield, and E. Wielandt, "A three-component borehole optical seismic and geodetic sensor," *Bull. Seismol. Soc. Amer.*, vol. 108, no. 4, pp. 2022–2031, Aug. 2018.
[18] W. Zhang, W. Huang, L. Li, W. Liu, and F. Li, "Fiber optic seismometer based on π-phase-shifted FBG and swept optical SSB-SC interrogation technique," in *Proc. 2nd Int. Conf. Fibre-Optic Photonic Sensors Ind. Saf. Appl. (OFSIS)*, Jan. 2017, pp. 21–26.
[19] W. Yuan, B. Pang, J. Bo, and X. Qian, "Fiber-optic sensor without polarization-induced signal fading," *Microw. Opt. Technol. Lett.*, vol. 56, no. 6, pp. 1307–1313, Jun. 2014.
[20] M. Pang, H. P. Zhou, M. Zhang, F. Lin, N. Zeng, and Y. B. Liao, "Analysis and amelioration about the cross-sensitivity of a fiber-optic accelerometer based on compliant cylinder," *J. Lightw. Technol.*, vol. 26, no. 3, pp. 365–372, Feb. 1, 2008.
[21] R. D. Pechstedt and D. A. Jackson, "Transducer mechanism of an optical fiber accelerometer based on a compliant cylinder design," *Proc. SPIE, Int. Soc. Opt. Eng.*, vol. 2360, pp. 380–383, Sep. 1994.
[22] W. Gao, J. Chen, Z. Ge, W. Sun, Q. Fu, J. Lang, T. Chang, and H.-L. Cui, "Calculation method for stiffness coefficient of compliant cylinder in fiber-optic interferometric vibration," *Chin. J. Lasers*, vol. 44, no. 3, pp. 256–262, Mar. 2017.
[23] J. Chen, "Research and design of fiber optic interferometric sea bottom seismic geophone," Ph.D. dissertation, College Instrum. Elect. Eng., Jilin Univ., Changchun, China, 2018.
[24] J. Chen, T. Chang, Y. Yang, W. Gao, Z. Wang, and H.-L. Cui, "Ultra-low-frequency tri-component fiber optic interferometric accelerometer," *IEEE Sensors J.*, vol. 18, no. 20, pp. 8367–8374, Oct. 15, 2018.
[25] J. Chen, T. Chang, Q. Fu, J. Lang, W. Gao, Z. Wang, M. Yu, and H.-L. Cui, "A fiber-optic interferometric tri-component geophone for ocean floor seismic monitoring," *Sensors*, vol. 17, no. 1, pp. 1125–1136, Jan. 2017.

YUE YANG received the B.S. degree from the College of Instrumentation and Electrical Engineering, Jilin University, in 2017, where she is currently pursuing the Ph.D. degree. Her research interests are fiber optical communications and sensing.

ZHONGMIN WANG received the B.S. degree in automation from the School of Electrical Engineering, University of Jinan, Jinan, China, in 2005, and the M.S. degree in control theory and control engineering from the College of Control Science and Engineering, Shandong University, Jinan, in 2008. He is currently pursuing the Ph.D. degree with the College of Instrumentation and Electrical Engineering, Jilin University, Changchun, China.

From 2009 to 2016, he was employed as an Assistant Researcher with the Shandong Academy of Sciences, China. His research efforts have been concentrated in the areas of optical fiber sensors and millimeter wave imaging.

TIANYING CHANG received the Ph.D. degree from the College of Control Science and Engineering, Shandong University, Jinan, China, in 2009.

From 2007 to 2008, she worked as a Joint Ph.D. student from the Stevens Institute of Technology. She was a Lecturer with Shandong University and a Postdoctoral Research Associate with New York University. She is currently an Associate Professor with Jilin University. Her research efforts have been concentrated in the areas of optical fiber sensors, THz systems, and nano-optics.

MIAO YU received the Ph.D. degree with the College of Instrumentation and Electrical Engineering, Jilin University, in 2017. He is currently a Lecturer with the University of Electronic Science and Technology of China, Zhongshan Institute. His research efforts have been concentrated in the areas of optical fiber sensing, weak signal detection and processing, pattern recognition.

JUNJIE CHEN received the B.S. degree from the College of Applied Geophysics, Changchun College of Geology, in 1989. He is currently a Senior Engineer with the Earthquake Administration Bureau of Jilin Province, China. His research interest is mainly focused on earthquake monitoring.

GUODONG ZHENG received the B.S. degree from the College of Communication Engineering, Jilin University, in 2005. He is currently an Engineer with the Earthquake Administration Bureau of Jilin Province, China. His research interest is mainly focused on earthquake monitoring.

HONG-LIANG CUI received the Ph.D. degree in theoretical physics from the Stevens Institute of Technology, in 1987. He was a professor of physics and engineering physics with the Stevens Institute of Technology, and a Professor of applied physics with New York University. He is currently a Professor of electrical engineering with Jilin University. His research efforts have been concentrated in the areas of solid-state electronics, fiber optical communications and sensing, high-frequency electromagnetic wave propagation and interaction with matter, and physics-based approaches to modeling of semiconductor and molecular devices.